Nonlinear Macromodeling of Voltage-Regulated Power Delivery Networks

Nonlinear macromodeling of voltage-regulated power delivery networks

Antonio Carlucci, Stefano Grivet-Talocia
Dept. Electronics and Telecommunications, Politecnico di Torino, Italy
antonio.carlucci@polito.it

***Abstract*—We introduce a frequency-domain macromodeling approach that generalizes Vector Fitting to mildly nonlinear systems, such as power delivery networks including integrated voltage regulators described by averaged models. The proposed approach overcomes the limitation of linearized descriptions, and leads to a black-box nonlinear macromodel of the entire power distribution network with drastically enhanced accuracy.**

I. Introduction

Modern power delivery architectures for high-end microprocessors rely on integrated buck converters to improve efficiency [1]. A typical power delivery network (PDN) topology, shown in Fig. 1, includes power converter stages between the *input* and *output network* blocks, which are both linear and passive. The power switches are driven by the duty cycle signals $d(t)$ produced by feedback compensators based on the deviation between the sensed load voltages $y(t)$ and a desired reference $y_{\rm ref}$.

In system-level power integrity (PI) analyses, the linear blocks are EM-accurate representations of all components and parasitics in the system (interconnects at board and package level, decaps, etc.), resulting in highly complex large-scale networks. This makes the transient analyses that are required in PI verification computationally demanding or even non-convergent. However, since only the load voltage responses $y(t)$ to current excitations $u(t)$ are of interest, a typical approach is to build a compact behavioral model of the u-y relation to reproduce the same *external* behavior as the original system, at a fraction of the computational cost. In absence of the voltage regulators, such u-y relation is linear and represented by the impedance matrix $Z(s)$ seen by the load. In such situation, compact models are typically obtained in a data-driven manner via off-the-shelf rational approximation algorithms such as Vector Fitting (VF) [2], [3].

The presence of DC-DC converters for local voltage regulation poses a challenge, because it introduces a weak nonlinearity, thus ruling out standard frequency-domain macromodeling approaches based on transfer function samples. This calls for a generalization to account for such nonlinear effects.

II. Problem statement and contribution

Following a standard practice in PI analysis, the power switches are here represented via averaged models. Under this assumption, we aim at building a behavioral model of the PDN including the converter stage and the linear blocks ($\mathcal{G}$, the dashed box in Fig. 1) and excluding the compensator. The input excitations to $\mathcal{G}$ are both $d(t)$ and $u(t)$. The feedback loop with the compensator will be reintroduced at runtime to evaluate $d(t)$ in real time.

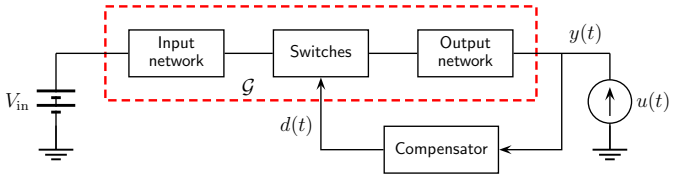

Fig. 1. Power Delivery Network topology. The dashed box encloses the target $\mathcal{G}$ of the proposed nonlinear macromodeling approach.

We choose Wiener-Hammerstein (W-H) model structure [4], [5] to represent the nonlinearity due to the power switches. Our main contribution is a novel modeling technique that combines VF with Harmonic Balance (HB) analysis [6] to identify a W-H model that accounts for nonlinear effects induced by $d(t)$. This can be seen as a nonlinear extension of VF for the adopted W-H topology. As for standard VF, model identification is performed in the frequency domain.

III. Formulation

A. Model structure

The proposed model $\mathcal{G}$ is built by augmenting a linear model $\mathcal{G}_{\rm lin}$ with a nonlinear correction $\mathcal{G}_{\rm nl}$ so that the overall model response is the sum of two components $y(t) = y_{\rm lin}(t) + y_{\rm nl}(t)$. The output $y_{\rm lin}(t)$ of $\mathcal{G}_{\rm lin}$ is the superposition of the effects due to d and u

$$y_{\rm lin}(t) = g_{{\rm lin},u}[u](t) + g_{{\rm lin},d}[d](t),$$

where the notation $g[u](t)$ indicates the response of the linear system g to the input u at time t, and capitalized G denotes its transfer function (TF). The linear block $\mathcal{G}_{\rm lin}$ has the following two-component TF

$$\mathbf{G}_{\rm lin}(\mathrm{j}\omega) = \begin{pmatrix} G_{{\rm lin},u}(\mathrm{j}\omega) & G_{{\rm lin},d}(\mathrm{j}\omega) \end{pmatrix}.$$

As for $\mathcal{G}_{\rm nl}$, we assume the W-H model structure shown in Fig. 2. Both u and d are first filtered by n linear systems to produce the signals $w_i[u]$, $w_i[d]$, $i = 1, \ldots, n$. Using vector notation, we define

$$\boldsymbol{w}[\star](t) = \begin{pmatrix} \star(t) & w_1[\star](t) & \cdots & w_n[\star](t) \end{pmatrix}^T \in \mathbb{R}^{n+1}$$

where $\star$ stands for either u or d. Next, the static nonlinearity in the middle forms the Kronecker products $\boldsymbol{w}[u] \otimes \boldsymbol{w}[d]$ and

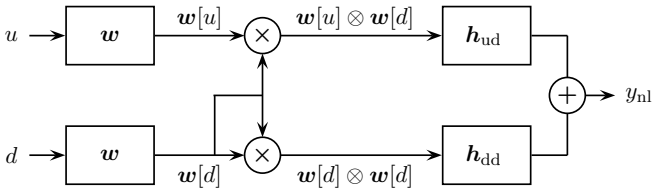

Fig. 2. Block schematic of the W-H model $\mathcal{G}_{\rm nl}$.

$\boldsymbol{w}[d]\otimes\boldsymbol{w}[d]$, giving rise, respectively, to a) an intermodulation product between d and u and b) second-order effects in d. Finally, the two linear blocks $\boldsymbol{h}_{ud}$ and $\boldsymbol{h}_{dd}$ map $(n+1)^2$ inputs into a single output, yielding

$$y_{\rm nl}(t) = \boldsymbol{h}_{ud}[\boldsymbol{w}[u]\otimes\boldsymbol{w}[d]] + \boldsymbol{h}_{dd}[\boldsymbol{w}[d]\otimes\boldsymbol{w}[d]].$$

In continuity with VF-based macromodeling, we adopt a frequency-domain approach in the characterization of $\mathcal{G}_{\rm nl}$ so as to obtain a model representation that is compatible with rational approximation tools. In particular, we consider the steady-state response of $\mathcal{G}_{\rm nl}$ under harmonic excitation as in [7], to define rational functions suitable to describe nonlinear effects. By setting $u(t) = e^{\mathrm{j}\omega_u t}$ and $d(t) = e^{\mathrm{j}\omega_d t}$ and propagating them through the blocks in Fig. 2, we see that the resulting $y_{\rm nl}(t)$ contains, among others, the intermodulation component $F_{ud}(\mathrm{j}\omega_u,\mathrm{j}\omega_d)e^{\mathrm{j}(\omega_u+\omega_d)t}$, with

$$F_{ud}(\mathrm{j}\omega_u,\mathrm{j}\omega_d) = \mathbf{H}_{ud}(\mathrm{j}\omega_u+\mathrm{j}\omega_d)\mathbf{W}_{ud}(\mathrm{j}\omega_u,\mathrm{j}\omega_d) \qquad (2)$$

where $\mathbf{W}_{ud}(\mathrm{j}\omega_u,\mathrm{j}\omega_d) = \mathbf{W}(\mathrm{j}\omega_u)\otimes\mathbf{W}(\mathrm{j}\omega_d)$. Similarly, to isolate the second-order effects in d, consider $u(t)=0$ and $d(t) = e^{\mathrm{j}\omega_1 t} + e^{\mathrm{j}\omega_2 t}$. In this case the output component at frequency $\omega_1+\omega_2$ is $F_{dd}(\mathrm{j}\omega_1,\mathrm{j}\omega_2)e^{\mathrm{j}(\omega_1+\omega_2)t}$, with

$$\begin{aligned} F_{dd}(\mathrm{j}\omega_1,\mathrm{j}\omega_2) = \mathbf{H}_{dd}(\mathrm{j}\omega_1+j\omega_2)\cdot \\ [\mathbf{W}(\mathrm{j}\omega_1)\otimes\mathbf{W}(\mathrm{j}\omega_2)+\mathbf{W}(\mathrm{j}\omega_2)\otimes\mathbf{W}(\mathrm{j}\omega_1)] \end{aligned} \qquad (3)$$

This simple analysis motivates using the bi-variate rational functions F_{ud} and F_{dd} to represent the W-H model $\mathcal{G}_{\rm nl}$.

B. Data collection

Regarding the linear part, we extract samples $\breve{\mathbf{G}}_{\rm lin}^{(k)} = \breve{\mathbf{G}}_{\rm lin}(\mathrm{j}\omega^{(k)})$, for $k=1,\dots,K$, using small-signal AC analysis around the nominal operating point. Note that, in the following, the accented symbol $\breve{x}$ indicates the observed or measured value of the quantity x. As for $\mathcal{G}_{\rm nl}$, two-tone HB analysis allows to extract the samples

$$\begin{aligned} \breve{F}_{ud}^{(k)} &= \breve{F}_{ud}(\mathrm{j}\omega_u^{(k)},\mathrm{j}\omega_d^{(k)}), \quad k=1,\dots,K_{ud} \\ \breve{F}_{dd}^{(k)} &= \breve{F}_{dd}(\mathrm{j}\omega_1^{(k)},\mathrm{j}\omega_2^{(k)}), \quad k=1,\dots,K_{dd} \end{aligned}$$

defined over two-dimensional frequency domains. In particular, $\breve{F}_{ud}^{(k)}$ is found by setting $u(t) = \cos(\omega_u^{(k)}t)$ and $d(t) = d_0+\alpha\cos(\omega_d^{(k)}t)$, with α chosen to keep the duty cycle in $[0,1]$. The resulting harmonic component at $\omega_u^{(k)}+\omega_d^{(k)}$ gives the result. Similarly, $\breve{F}_{dd}^{(k)}$ is extracted by HB with $d(t) = d_0+\alpha\cos(\omega_1^{(k)}t)+\alpha\cos(\omega_2^{(k)}t)$.

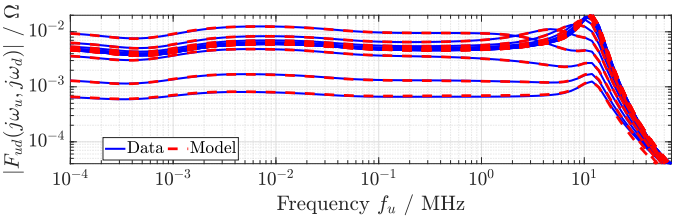

Fig. 3. Model-data comparison of the bi-variate function $F_{ud}(\mathrm{j}\omega_d,\mathrm{j}\omega_u)$. Different curves correspond to several fixed values of ω_d. Similar results hold for F_{dd}.

C. Rational approximation

Using the above-defined data, the behavioral model can be built using rational approximation. In fact, a direct application of VF to $\breve{\mathbf{G}}_{\rm lin}^{(k)}$ gives a TF model in pole-residue form

$$\mathbf{G}_{\rm lin}(s) = \sum_{\ell=1}^{\nu}\mathbf{R}_{{\rm lin},\ell}(s-p_\ell)^{-1}$$

where $p_\ell\in\mathbb{C}$ are ν poles and $\mathbf{R}_{{\rm lin},\ell}\in\mathbb{C}^{1\times 2}$ the corresponding residues. Once the (linearized) system poles p_ℓ have been identified through VF, we assume these are sufficient to describe the whole system dynamics. This simplifies the problem of building models of $\mathbf{W}(s)$, $\mathbf{H}_{ud}(s)$, $\mathbf{H}_{dd}(s)$ because we take them to be rational functions with the same poles. The next observation is that there is no further loss of generality in assuming that $\mathbf{W}(s)$ coincides with the partial fraction basis

$$\mathbf{W}(s) = \begin{pmatrix}1 & (s-p_1)^{-1} & \cdots & (s-p_\nu)^{-1}\end{pmatrix}^T.$$

Hence, the only quantities to be estimated are the residues of $\mathbf{H}_{ud}(s)$, $\mathbf{H}_{dd}(s)$, which have pole-residue expansions

$$\mathbf{H}_\star(s) = \sum_{\ell=1}^{\nu}\mathbf{T}_{\star,\ell}(s-p_\ell)^{-1}, \quad \star=\{dd,ud\} \qquad (4)$$

where $\mathbf{T}_{\star,\ell}\in\mathbb{C}^{1\times(n+1)^2}$. Then, (2) and (4) imply that matching F_{ud} to the sampled data $\breve{F}_{ud}$ translates in the approximation

$$\sum_{\ell=1}^{\nu}[\mathrm{j}(\omega_u^{(k)}+\omega_d^{(k)})-p_\ell]^{-1}\mathbf{T}_{ud,\ell}\mathbf{W}_{ud}(\mathrm{j}\omega_u^{(k)},\mathrm{j}\omega_d^{(k)}) \approx \breve{F}_{ud}^{(k)}$$

that is a linear least-squares problem in the unknowns $\mathbf{T}_{ud,\ell}$. The residues $\mathbf{T}_{dd,\ell}$ are found analogously by optimizing the approximation $F_{dd}\approx\breve{F}_{dd}$ and using (3)–(4).

IV. Numerical results

The proposed model is tested on a single-core version of the multicore PDN described in [8], which refers to an Intel-based mobile architecture. We sampled all transfer functions by sweeping the frequency of the load current excitation u and that of the duty cycle d up to 0.5 GHz. In total, $K=120$, $K_{dd}=10^4$, $K_{ud}=1.2\cdot10^4$ samples were collected. We used $\nu=12$ poles to fit the bi-variate models, obtaining the results reported in Fig. 3.

In time domain, the model was tested with two load current signals. The first is a $3\,\mu$s long ramp-up analysis using a

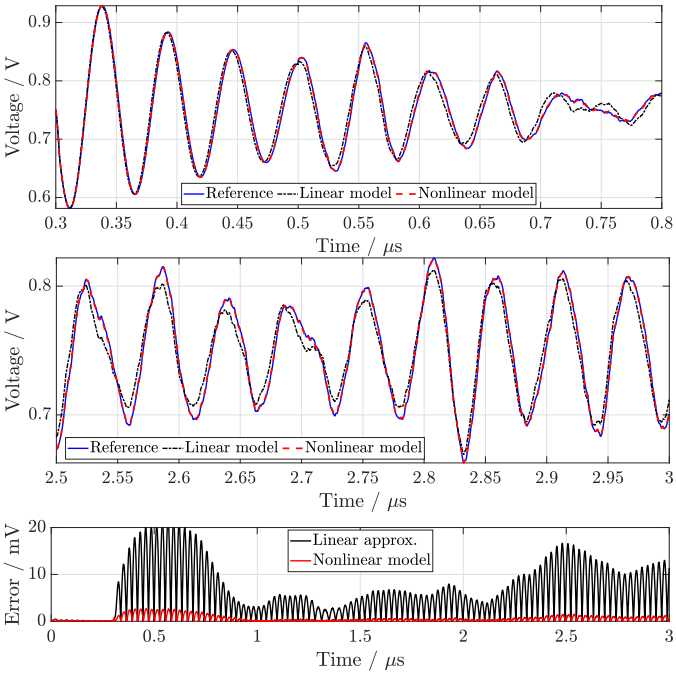

Fig. 4. Transient response comparing the reference with linear and nonlinear models. Top: subinterval $t \in [0.3, 0.8]\,\mu$s, i.e. response to noisy current step. Middle: response in the interval $[2.5, 3]\,\mu$s. Bottom: instantaneous error along the entire simulation.

10 A current step occurring at $t = 0.3\,\mu$s with 3 ns rise time. This is superimposed to a filtered white noise with bandwidth $[4, 16]$ MHz (close to the peak in Fig. 3) and peak amplitude equal to 2 A. The model response is compared to the reference in Fig. 4, showing the detail of the step response in the top panel, and the response to noise in the middle panel. A quantitative error analysis comparing both linear and nonlinear model responses with the reference along the entire simulation interval is also reported in Fig. 4 (bottom panel). Solving the proposed model in MATLAB for 5×10^4 fixed-length timesteps takes 2.7 s, whereas the same simulation of the original system requires 191 s. The proposed algorithm runs in about 63 s, whereas data collection via HB takes 1.2 hours in our experiments. It is important to remark that the benefit of this modeling approach is also that it captures nonlinear effects that would be impossible to model through linear macromodeling. This is evident in Fig. 5, which shows that the RMS error of the linear model remains almost constant as the number of poles ν is increased, while the nonlinear model provides higher accuracy because the additional model poles improve the approximation of higher-order effects that are structurally neglected with a linear approximation.

The second test signal is reported in Fig. 6 (top panel). It consists of a sequence of steps that sequentially shift the operating point of the load current from 0 A to 10 A every 0.5μs, in discrete steps. This is superimposed to a chirp signal of amplitude 1 A that repeatedly sweeps from 5 to 25 MHz. As the average load current departs from zero (that is the operating point used to construct the small-signal model $\mathcal{G}_{\text{lin}}$),

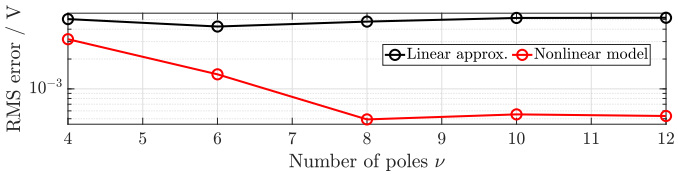

Fig. 5. RMS error comparison between a small-signal (linear) model and the proposed nonlinear model, reported by increasing the number of model poles.

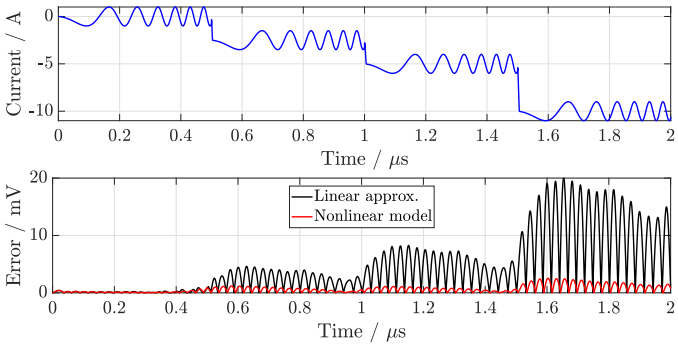

Fig. 6. Transient simulation using a chirp signal around several bias levels. Top panel: load current excitation. Bottom panel: instantaneous error.

the linear approximation becomes increasingly inaccurate. Adding the second-order nonlinear corrections decreases this error by at least one order of magnitude.

V. Conclusion

This paper has demonstrated that, in presence of integrated voltage regulators, linearized models of the PDN impedance may be inadequate to reproduce with sufficient accuracy the transient load voltages. The proposed approach, which extends Vector Fitting to account for the nonlinear terms that are induced by the regulator switches, is able to correct the linearized impedance model to represent, as a black-box, the entire voltage-regulated PDN structure.

References

[1] E. A. Burton *et al.*, "FIVR — Fully integrated voltage regulators on 4th generation Intel® Core™ SoCs," in *2014 IEEE Applied Power Electronics Conference and Exposition*, Mar. 2014, pp. 432–439.

[2] B. Gustavsen and A. Semlyen, "Rational approximation of frequency domain responses by vector fitting," *IEEE Transactions on Power Delivery*, vol. 14, no. 3, pp. 1052–1061, 1999.

[3] S. Grivet-Talocia and B. Gustavsen, *Passive macromodeling: Theory and applications*. John Wiley & Sons, 2015.

[4] E.-W. Bai and F. Giri, *Introduction to Block-oriented Nonlinear Systems*. London: Springer London, 2010, pp. 3–11.

[5] J. A. Oliver, R. Prieto, J. A. Cobos, O. Garcia, and P. Alou, "Hybrid wiener-hammerstein structure for grey-box modeling of DC-DC converters," in *2009 Twenty-Fourth Annual IEEE Applied Power Electronics Conference and Exposition*, 2009, pp. 280–285.

[6] R. J. Gilmore and M. B. Steer, "Nonlinear circuit analysis using the method of harmonic balance—a review of the art. part i. introductory concepts," *International Journal of Microwave and Millimeter-Wave Computer-Aided Engineering*, vol. 1, no. 1, pp. 22–37, 1991.

[7] S. Baumgartner and W. Rugh, "Complete identification of a class of nonlinear systems from steady-state frequency response," *IEEE Transactions on Circuits and Systems*, vol. 22, no. 9, pp. 753–759, 1975.

[8] A. Carlucci, S. Grivet-Talocia, S. Kulasekaran, and K. Radhakrishnan, "Structured model order reduction of system-level power delivery networks," *IEEE Access*, vol. 12, pp. 18 198–18 214, 2024.